

Investigation of detection limits of ZnSe and Cu₂SnSe₃ secondary phases in Cu₂ZnSnSe₄

Galina Gurieva*¹, Sergiu Levenco¹, Afonso Pereira Correia de Sousa^{1,2},

Thomas Unold¹ and Susan Schorr^{1,3}

¹ Helmholtz Zentrum Berlin für Materialien und Energie GmbH, Hahn-Meitner-Platz 1, 14109, Berlin, Germany

² Universidade de Coimbra, Physics Department, Palácio dos Grilos Rua da Ilha 3000-214 Coimbra, Portugal

³ Free University Berlin, Institute of Geological Sciences, Malteserstr. 74-100, Berlin, Germany

Quaternary Cu₂ZnSnSe₄ (CZTSe) is a promising semiconductor material for absorber layers in thin film solar cells. Nevertheless, a low open circuit voltage with respect to the band gap energy is a common phenomenon in CZTSe-based photovoltaic devices, which may be caused by compositional and phase inhomogeneities of the absorber layer. The detection limit of conventionally used characterization methods for secondary phases in such absorber layers is still under discussion. In this work the limits of the sensitivity of X-ray diffraction and Raman spectroscopy to the presence of two very common for Cu₂ZnSnSe₄ secondary phases, ZnSe and Cu₂SnSe₃, are examined.

1 Introduction

Copper zinc tin selenide (CZTSe) has been emerging as an important light absorbing material consisting of cheap and earth-abundant constituents. CZTSe is a promising semiconductor material due to its properties – the direct band gap around 1 eV and high absorption coefficient ($> 10^4 \text{ cm}^{-1}$) [1-3]. The highest conversion efficiency of CZTSe solar cells is above 11.6% [3,4].

Despite those promising results there are still a number of challenges that are needed to be faced in order to achieve high quality efficient solar cells. A low open circuit voltage with respect to the band gap is a common phenomenon in CZTSe-based photovoltaic devices. A plausible reason for this is a reduction in the effective band gap due to inhomogeneities in structural parameters and composition of the absorber layer, the occurrence of secondary phases as well as a non-ideal photovoltaic device structure [5]. Deviations from stoichiometry in CZTSe are leading to variations of structural parameters and the formation of intrinsic point defects which significantly influence the electrical and optical properties of the material [6, 7]. But stoichiometry deviations are not the only challenge which has to be faced. It seems to be extremely difficult to produce single phase CZTSe thin film, as a result the undesired formation of secondary phases is inevitable. The detection and quantification of these secondary phases is extremely important and to gain valid information on the influence of phase inhomogeneities on the performance of solar cells remains challenging. In order to achieve this goal the understanding of detection limits of conventionally used characterization methods is essential. The aim of this work is to study the sensitivity limits of X-ray diffraction and Raman spectroscopy to the presence of two very common in Cu₂ZnSnSe₄ secondary phases ZnSe and Cu₂SnSe₃.

2 Experimental

To achieve the main purpose of this work, two sets of powder samples were prepared. In order to “simulate” a secondary phase containing CZTSe absorber, a single phase CZTSe powder was mixed with a given amount of “secondary phase” (single phase ZnSe or CTSe powder), in order to obtain a calibration like series like set of samples containing 1%, 2%, 3%, 5%, 10% and 20% mixtures of the main phase and secondary phase.

The single phase $\text{Cu}_2\text{ZnSnSe}_4$ (CZTSe) powder samples were synthesized by solid state reaction of the pure elements, as described earlier in [8, 9]. The ZnSe and CTSe powder samples use as secondary phases were synthesized by the same method, but with an optimized process. For the ZnSe powder synthesis 5N pure starting materials were used as well, but due to the very fast reaction of Zn with Se it was very important to maximize the surface of the Zn source, in order to obtain the homogenous ZnSe and not a Zn pellet covered with a very thin ZnSe layer. To overcome this problem Zn in form of shavings was used. It allowed us to obtain homogenous ZnSe powder in only one synthesis step. The Cu_2SnSe_3 (CTSe) powder was prepared the same way as the CZTSe powders, but with a slightly lower maximum growing temperature (700°C). Two annealing periods with a homogenization step in between were applied in this case as well.

Table 1 Overview of synthesized samples: cation ratios Cu/(Zn+Sn) and Zn/Sn obtained from the WDX analysis, chemical formula, off-stoichiometry type.

Sample Name	Cu/Zn+Sn	Zn/Sn	Type	Formula
ZnSe	0.000	1.000		ZnSe
CTSe	2.000	0.000		Cu_2SnSe_3
CZTSe - I	1.000	1.053	B-G	$\text{Cu}_{1.98}\text{Zn}_{1.04}\text{Sn}_{0.98}\text{Se}_4$
CZTSe - II	0.981	1.055	G-F	$\text{Cu}_{2.01}\text{Zn}_{1.03}\text{Sn}_{0.98}\text{Se}_4$

In order to determine the chemical composition of the four powder samples, wavelength dispersive X-ray spectroscopy (WDX) has been performed using an electron microprobe analysis system. Figure 1 (bottom) presents a back scatter electron (BSE) micrograph showing the homogeneity of one of the CZTSe samples. To gain reliable results from the WDX measurements, the system was calibrated using elemental standards. High accuracy of the compositional parameters was achieved by averaging over 20 local measurement points within one grain and averaging over more than 30 grains of the ZnSe, CTSe or CZTSe phase. The result of this compositional and phase analysis proved the synthesis of homogeneous, single phase stoichiometric ZnSe and CTSe powders. In case of the two CZTSe powders, they were both homogeneous and single phase, but with slightly off-stoichiometric composition. Both of the samples were slightly Zn rich and Sn poor, but while CZTSe-I was also slightly Cu poor, CZTSe-II was very close to stoichiometry, concerning the Cu content. The Cu/(Zn+Sn) and Zn/Sn ratios of the samples as well as the off-stoichiometry type information and final formulae of the compounds, calculated according to the method described in [10], are presented in Table I.

Table 2 Planned versus obtained percentages of “secondary phases” in the resulting mixtures.

Planned %	Obtained %	
	ZnSe	CTSe
20	20.10(2)	19.26(2)
10	10.05(1)	9.64(1)
5	5.01(1)	4.50(1)
3	3.10(1)	2.78(1)
2	2.01(1)	1.58(1)
1	1.01(1)	1.17(1)

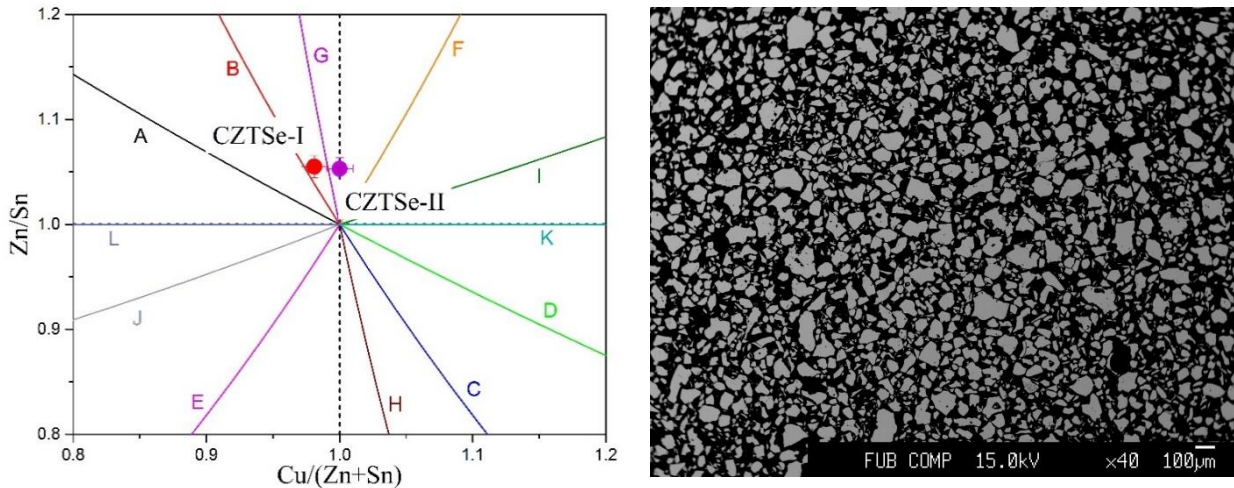


Figure 1 left) off-stoichiometric CZTSe cation ratio plot; right) backscattered electron micrographs of off-stoichiometric CZTSe-I, CZTSe detected in grey grains. Black background is the epoxy matrix.

As the next step the two CZTSe samples were mixed with the “secondary phase” powders to simulate a mixture of main phase and secondary phases in an absorber layer. CZTSe-I was mixed with ZnSe, while CZTSe-II was mixed with CTSe. The amounts necessary to produce 1g of mixture were weighted and the powders were mixed in order to obtain 1%, 2%, 3%, 5%, 10% and 20% mixtures of CZTSe-I with ZnSe and CZTSe-II with CTSe respectively. Additional manual grinding of these mixtures in agate mortar was applied in order to enhance the homogeneous distribution of the secondary phase within CZTSe powder without influencing any of the phase compositions. The obtained percentages versus the planned are shown in Table II.

The first method applied was the X-ray powder diffraction (PXRD). Powder X-ray diffraction data of all four phase pure powders as well as all of the mixtures were collected at room temperature using a PANalytical X'pertPro MPD diffractometer equipped with $\text{CuK}\alpha$ radiation ($\lambda=1.54056 \text{ \AA}$) in a focusing Bragg-Brentano geometry. Rietveld refinement of diffraction data was performed, paying a special attention to features arising from ZnSe and Cu_2SnSe_3 in the mixed sample series. The refinement procedure was started with the data of the single phase powder samples (CZTSe-I, CZTSe-II, ZnSe and CTSe) following the route described in [9] using the FullProf software package [11]. For the XRD data analysis of the mixtures, the same route as in case of pure materials was applied, but the values for structural parameters as well as peak shape parameters are taken from the refinements of the pure samples. The only parameters refined for the mixtures are zero shift, the scale factor and the background. The amounts (weight%) of secondary phases determined by Rietveld analysis have been compared with the initial values (weight in), determining in this way the detection limits of PXRD for these secondary phases.

To study the crystal structure of the synthesized mixtures at the micrometer scale Raman spectroscopy has been employed. The Raman measurements are carried out in the backscattering configuration using a Horiba HR800 setup equipped with a 632.8 nm He-Ne laser and Olympus objective (NA=0.1). The power used was 1.4 mW and a spot size of about 3 μm in diameter was applied. The spectra were corrected with 632.3nm and 640.2nm lines of the calibrated lamp.

3 Results and discussion

In the first approach to the problem of the detection limits determination, the XRD pattern were checked if there are any visible differences, when comparing the mixtures to the pure CZTSe. As it can be observed in Figure 2 (top), the presence of ZnSe is clearly noticeable starting with 10% ZnSe (features corresponding to the ZnSe secondary phase are marked with arrows). Because in an absorber layer compositional variations of the CZTSe phase may occur which cause variations in the lattice parameter and thus shifts in the Bragg peaks, XRD pattern have been simulated to prove the visibility of the Bragg peaks arising from the ZnSe secondary

phase. In these simulations experimentally obtained lattice parameters for off-stoichiometric CZTSe [ref.] have been used and a mixture of 20%ZnSe has been applied. Assuming comparable instrumental resolutions it can be shown, that a small feature arising from the ZnSe secondary phase is also visible for different off stoichiometric CZTSe main phases. Unfortunately in case of CZTSe-II- CTSe mixtures, the visual difference was not that easy to determine.

Comparing the results of Rietveld analysis concerning the amounts of secondary phases with the initial values of the calibration series (Table 3 and Figure 3), though shows a different result for the both applied secondary phases. We can assume that in the Rietveld analysis the fraction of ZnSe is clearly underestimated, most probably due to the strong overlap of the CZTSe Bragg peaks with the ZnSe peaks.

In case of the mixtures with CTSe as secondary phase the results of the Rietveld analysis are much more promising, as it can be seen in the Figure 3. While once again for mixtures with a secondary phase concentrations of 3% or less, the results are not very reliable, the values for the mixture corresponding to 5% of secondary phase and higher are quite close to the expected values.

Table 3 Comparison of amounts (weight %) obtained for the “secondary phase” content in the mixtures by XRD with the initial (weight in) values.

ZnSe real (%)	XRD (%)	CTSe real (%)	XRD (%)
20.10(2)	3.56(3)	19.26(2)	12.48(24)
10.05(1)	1.26(2)	9.64(1)	10.48(19)
5.01(1)	0.58(1)	4.50(1)	5.17(9)
3.10(1)	0.58(1)	2.78(1)	1.72(5)
2.01(1)	0.13(1)	1.58(1)	2.16(1)
1.01(1)	0.00(1)	1.17(1)	0.63(1)

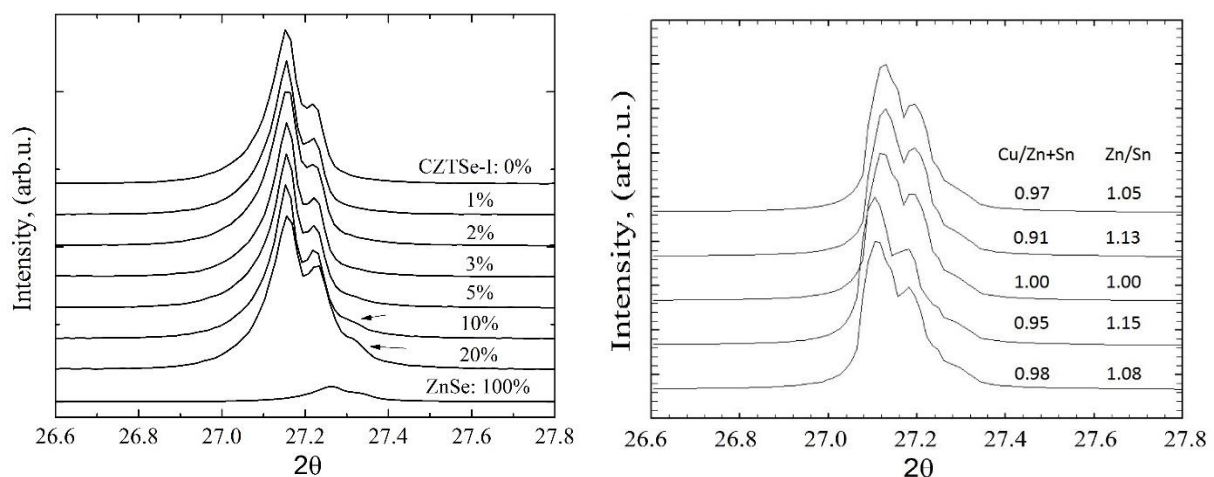


Figure 2 left) Zoom in of 112 peak of the CZTSe-I –ZnSe mixtures; right) Simulation of the 20% ZnSe mixture, using different compositions of CZTSe phase

Figure 4 shows Raman spectra of CZTSe-I and CZTSe-II powders mixed with different amount of the ZnSe and CTSe secondary phases, respectively. For a better comparison the characteristic Raman spectra of the pure secondary phase samples ZnSe and CTSe are also plotted. To exclude influence from the bigger grains in the mixtures each spectrum on the graph represents an average signal from several distant ($>100\ \mu\text{m}$) points.

With increase of the CTSe phase content a reduction of the dip amplitude between two main kesterite A-modes at 172 and $196\ \text{cm}^{-1}$ [12] can be observed, which is attributed to the contribution of the dominant CTSe mode at $180\ \text{cm}^{-1}$ [13]. In an extended measurement (~ 300 points) on the 20% CTSe mixture no single spot with a clear signal at $180\ \text{cm}^{-1}$ could be detected. Therefore, these data indicate that the Raman scattering efficiency of the CTSe phase is lower than of the kesterite type CZTSe main phase as an absence of CTSe in the large scanned area is very unlikely. In contrast, at the highest ZnSe concentration a characteristic ZnSe mode at $252\ \text{cm}^{-1}$ [14] can be well resolved in the spectrum of the mixture. Moreover, some single points taken on the 10% ZnSe mixture show an intensity increase in this high frequency region, too. For lower ZnSe concentrations the spectra are nearly identical and similar to the Raman spectrum of the pure CZTSe phase. Investigations on the extended sample areas (~ 300 points) allowed finding few points showing a ZnSe mode in in the 3% and 5% concentrations mixtures, but no such points were seen in 1 and 2% ZnSe mixtures. Following a recently proposed approach based on the ratio of the ZnSe mode to the kesterite mode at $235\ \text{cm}^{-1}$ [15], the the number of ZnSe containing measured points for the 3 and 5% ZnSe mixtures can be further increased., On the other hand this is not possible for measurements of mixtures with less than 3% ZnSe.. The usage of a $457.9\ \text{nm}$ laser line, corresponding to the resonant conditions for the ZnSe phase [15], or measurements over larger areas of the sample, would help to resolve the ZnSe phase in these mixtures.

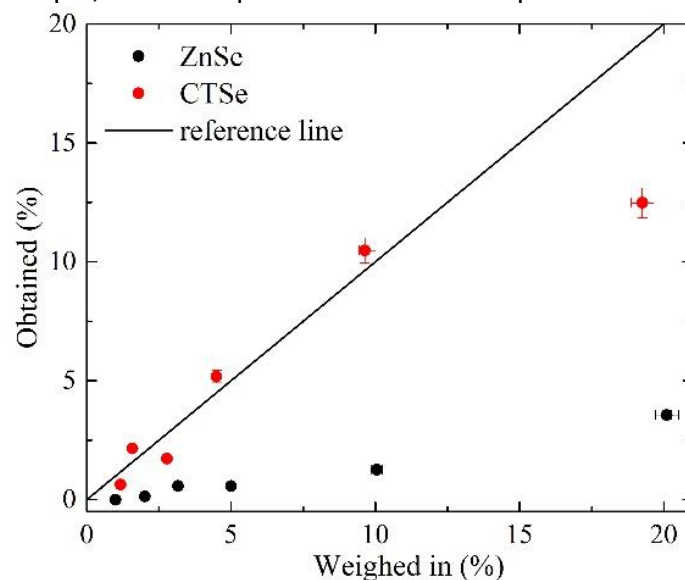


Figure 3 Comparison between the percentages of secondary phase obtained by XRD for ZnSe (black) and CTSe (red).

Finally, a possible qualitative determination of ZnSe and CTSe phases from the Raman data deserve an important comment. Since the Raman scattering intensity is directly proportional to the scattered volume, intensity changes could be directly linked to variations in the amount of the secondary phase under assumption of the similar Raman cross section for the different phases. On the other hand, the scattered volume depends on the penetration depth of the focused laser light, which is inversely proportional to the absorption coefficient, α , at the

photon energy corresponding to the laser line. It is known from the optical measurements that α_{CTSe} is higher than α_{CZTSe} at 1.96 eV by a factor of ~ 1.5 [16]. However, α_{CZTSe} is higher by factor of 10 or more than α_{ZnSe} [17] and, thus, corrections to the actual thickness of the ZnSe grains would be strongly required in the qualitative determination of the ZnSe phase content.

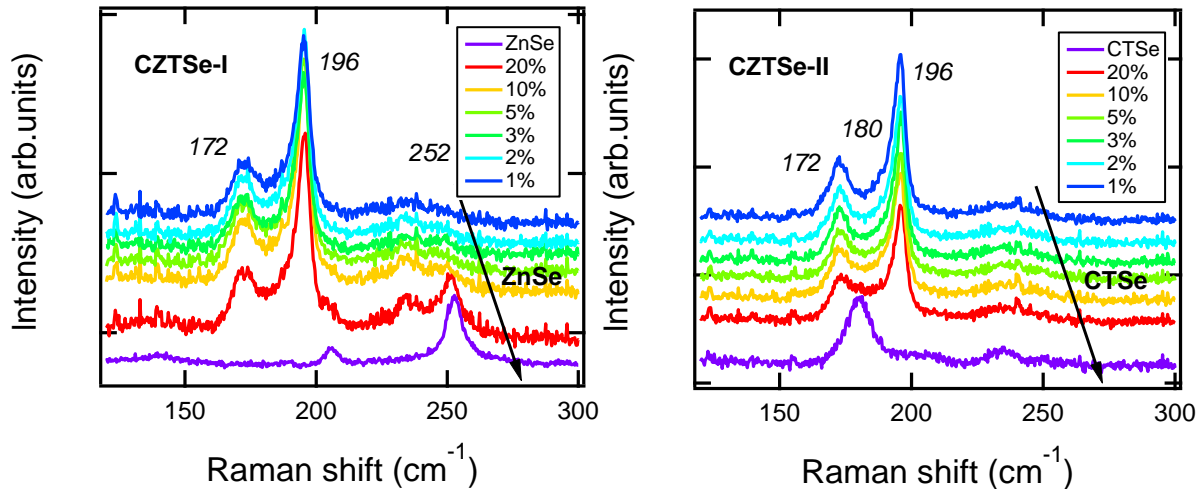


Figure 4 Comparison between the Raman spectra of CZTSe-I and CZTSe-II mixtures with 1%-20% addition percentages of the secondary phases: top) ZnSe; bottom) CTSe.

4 Conclusions

With this work it can be concluded that the detection limit for ZnSe as secondary phases in CZTSe for the X-ray diffraction is located between concentrations of 3 and 5 %, as the Bragg peaks of ZnSe are already visible for amounts of $>5\%$. Nevertheless the quantitative results of the Rietveld analysis for concentrations below 5% are not reliable. It is important to notice that for the mixtures with ZnSe the Rietveld analysis underestimates the presence of the secondary phase by a factor of at least 6, while for CTSe there is a reasonable agreement with the expected values of the calibration series. Using Raman spectroscopy it was possible to detect the ZnSe phase via its characteristic 252 cm^{-1} mode down to 3% concentration. In case of CTSe as secondary phase the sensitivity results on its detection were inconclusive, which can be related to its lower Raman cross section in comparison to the kesterite host phase.

Acknowledgements Financial supports from KESTCELLS 316488, FP7-PEOPLE-2012 ITN, Multi-ITN project is acknowledged.

References

- [1] León, M., et al., *Spectroscopic ellipsometry study of $\text{Cu}_2\text{ZnSnSe}_4$ bulk crystals*. Applied Physics Letters, 2014. **105**(6): p. 061909.
- [2] Ahn, S., et al., *Determination of band gap energy (E_g) of $\text{Cu}_2\text{ZnSnSe}_4$ thin films: On the discrepancies of reported band gap values*. Applied Physics Letters, 2010. **97**(2): p. 021905.
- [3] Gütay, L., et al., *Lone conduction band in $\text{Cu}_2\text{ZnSnSe}_4$* . Applied Physics Letters, 2012. **100**(10): p. 102113.
- [4] Lee, Y.S., et al., *$\text{Cu}_2\text{ZnSnSe}_4$ Thin-Film Solar Cells by Thermal Co-evaporation with 11.6% Efficiency and Improved Minority Carrier Diffusion Length*. Advanced Energy Materials, 2015. **5**(7)

- [5] X. Liu et al., *The current status and future prospects of kesterite solar cells: a brief review*, Prog. Photovolt: Res. Appl, 2016, **24**: 879–898
- [6] Chen, S., et al., *Classification of Lattice Defects in the Kesterite $\text{Cu}_2\text{ZnSnS}_4$ and $\text{Cu}_2\text{ZnSnSe}_4$ Earth-Abundant Solar Cell Absorbers*. Advanced Materials, 2013. **25**(11): p. 1522-1539.
- [7] Gershon, T., et al., *Photovoltaic Materials and Devices Based on the Alloyed Kesterite Absorber $(\text{Ag}_x\text{Cu}_{1-x})_2\text{ZnSnSe}_4$* . Advanced Energy Materials, 2016.
- [8] Gurieva, G., et al., *Structural characterisation of $\text{Cu}_{2.04}\text{Zn}_{0.91}\text{Sn}_{1.05}\text{S}_{2.08}\text{Se}_{1.92}$* . physica status solidi (c), 2015. **12**(6): p. 588-591.
- [9] Valle Rios, L.E., et al., *Existence of off-stoichiometric single phase kesterite*. Journal of Alloys and Compounds, 2016. **657**: p. 408-413.
- [10] R.Gunder, G. Gurieva, J. Marques-Prieto, S. Schorr, J. Alloys and Coump. To be subbmitted
- [11] Juan Rodriguez-Carvajal and Thierry Roisnel, www.ill.eu/sites/fullprof/
- [12] M. Guc et al, *Polarized Raman scattering analysis of $\text{Cu}_2\text{ZnSnSe}_4$ and $\text{Cu}_2\text{ZnGeSe}_4$ single crystals* J. Appl. Phys., 2013, **114**: 193514.
- [13] G. Marcano et al, *Raman spectrum of monoclinic semiconductor CuSnSe* , Solid State Communications, 2011, **151**: 84–86
- [14] G. Perna et al, *Temperature dependence of the optical properties of ZnSe films deposited on quartz substrate*, Appl. Phys. A, 2006, **83**: 127.
- [15] R. Djemour et al, *Multiple phases of $\text{Cu}_2\text{ZnSnSe}_4$ detected by room temperature photoluminescence*, Applied Physics Letters, 2013. **102**: p. 222108.
- [16] Y. Hirate et al, *Quantitative determination of optical and recombination losses in thin-film photovoltaic devices based on external quantum efficiency analysis*, J. Appl. Phys., 2015, **117**: 015702.
- [17] M. El Sherif et al, *Optical characteristics of thin ZnSe films of different thicknesses*, J. Mater. Sci—Mater. Electron, 1996, **7** (6): p. 391.